

Fabrication and evaluation of Si_xN_y coatings for total joint replacements

J. Olofsson · M. Pettersson · N. Teuscher ·
A. Heilmann · K. Larsson · K. Grandfield ·
C. Persson · S. Jacobson · H. Engqvist

Received: 6 January 2012 / Accepted: 17 March 2012 / Published online: 12 June 2012
© Springer Science+Business Media, LLC 2012

Abstract Wear particles from the bearing surfaces of joint implants are one of the main limiting factors for total implant longevity. Si_3N_4 is a potential wear resistant alternative for total joint replacements. In this study, Si_xN_y -coatings were deposited on cobalt chromium-discs and Si-wafers by a physical vapour deposition process. The tribological properties, as well as surface appearance, chemical composition, phase composition, structure and hardness of these coatings were analysed. The coatings were found to be amorphous or nanocrystalline, with a hardness and coefficient of friction against Si_3N_4 similar to that found for bulk Si_3N_4 . The low wear rate of the coatings indicates that they have a potential as bearing surfaces of joint replacements. The adhesion to the substrates remains to be improved.

1 Introduction

Total joint replacements have a longevity of about 15 years [1]. Due to increasing numbers of younger patients receiving implants and an aging population, implant longevity must increase to reduce the number of revisions. Often, it is the wear particles produced rather than the

material loss from the joint surfaces that become a limiting factor. These wear particles may cause inflammation and osteolysis which leads to degeneration of the bone and eventually loosening of the implant [1–3].

The bearing surfaces of the total hip joint replacements of today commonly consist of a cobalt chromium (CoCr) head that slides against a ultra-high-molecular-weight polyethylene (UHMWPE) liner. The wear particles produced in the system consist primarily of UHMWPE [4, 5]. Alternative material combinations are used to reduce particle generation, for example CoCr against CoCr or against ceramic materials like alumina (Al_2O_3) and zirconia (ZrO_2). Also metal and ceramic particles have been shown to cause osteolysis, however submicron UHMWPE—particles are considered the biologically most active debris [3]. For metal on metal prostheses, it has been demonstrated that corrosion of metal wear particles increases the amount of metal ions in the body. This is a cause for concern considering Co and Cr ions are known carcinogens [6]. Ceramics, in general, are less prone to corrosion, have lower wear rates and produce less wear particles [5, 7, 8]. However, a disadvantage of alumina and zirconia in comparison to metals is that they are relatively brittle in bulk form, which could lead to catastrophic failure in vivo. Alternative ceramics that have shown potential include silicon nitride (Si_3N_4) which has a higher fracture toughness than alumina and also has demonstrated superior results in rolling contact fatigue tests [9, 10]. Previous investigations have shown that silicon nitride dissolves in phosphate buffered saline (PBS) and is predicted to dissolve in vivo [11]. Furthermore, the Si^{4+} ions that may be extracted from Si_3N_4 eventually excrete in the urine [12]. Tribological tests of silicon nitride sliding against silicon nitride exhibit low wear and a low coefficient of friction in water, PBS, or bovine serum solution [11, 13]. It has also

J. Olofsson (✉) · M. Pettersson · K. Grandfield · C. Persson ·
S. Jacobson · H. Engqvist
Applied Materials Science, Uppsala University, Uppsala,
Sweden
e-mail: johanna.olof@gmail.com

N. Teuscher · A. Heilmann
Fraunhofer Institute for Mechanics of Materials IWM, Halle,
Germany

K. Larsson
Materials Chemistry, Uppsala University, Uppsala, Sweden

been reported that silicon nitride dissolves in water during friction, producing smooth surfaces under the tribochemical wear and leaving no solid wear particles behind [14]. Other authors claim that the wear particles that are produced when Si_3N_4 slides against Si_3N_4 in water often consists of silica (SiO_2) and are mainly amorphous [13].

One advantage of ceramic coatings on metal substrates is the good resistance to mechanical stresses offered by the combination of a ductile substrate and a hard wear-resistant surface. Ceramic coatings on metal substrates have therefore been suggested for the bearing components of joint replacements, including coatings of titanium nitride (TiN), diamond like carbon (DLC), chromium nitride (CrN), chromium carbon nitride (CrCN) and zirconium oxide (ZrO_2) [15–18]. Deposition processes for silicon nitride coatings for biomedical and other applications outside human body have also been described [19–22]. These processes include chemical vapour deposition (CVD) [20], ion-assisted deposition (IAD) [23], plasma immersion ion implantation and deposition (MPIID) [19], physical vapour deposition (PVD) [21, 22] and plasma spray coating techniques [24]. Each technique exhibits advantages and disadvantages, for example plasma sprayed coatings present poor adhesion to the substrate while silicon nitride films produced with CVD results in hydrogenated films [16, 22]. PVD has limitations when it comes to get an evenly distributed coating over complex shapes (line-of-sight process). The PVD process has been chosen for the present study due to its ability to produce versatile coating compositions while maintaining a relatively low substrate temperature.

Density functional theory (DFT) calculations have been applied to provide insight into the optimal composition of the coating for stability and reactivity *in vivo*.

Wear resistant bearing surfaces, causing a minimum amount wear particles and where these particles are resorbable, are predicted to reduce the risk of implant loosening, thereby extending the life span of hip joint implant. The aim of this work was to manufacture and evaluate such Si_3N_4 coatings on a CoCr substrate.

2 Experimental

2.1 Theoretical modelling

The effect on particle stability and surface reactivity from doping C into Si_3N_4 has been theoretically investigated using DFT calculations under periodic boundary conditions. The Generalized Gradient Approximation (GGA-PW91) developed by Perdew and Wang [25], was used in describing the electronic exchange and correlation interactions. The kinetic energy cut off was set to 240 eV in the

plane wave function description, and a Monkhorst–Pack generated k-point mesh was used for all calculations [26]. The main goal with these calculations was to find the optimal C dopant concentration for which possible fragments of Si_3N_4 will be resorbed more rapidly. To be able to approximate the effect of dopant element on the chemical stability, the effect of C concentration on the formation energy of the whole system (i.e. bulk Si_3N_4 with substitutional C) has been calculated. We will hereby be able to identify the effect of C on the energetic stability of the system. As a measure of Si_3N_4 surface reactivity, we have calculated the adsorption energy of H and OH, respectively, since water molecules will most often chemisorb dissociatively to a reactive surface.

2.2 Coating deposition

The Si_xN_y -coatings were deposited on a CoCr substrate of type ASTM F1537 and also on silicon wafers. The CoCr substrates were polished to a surface roughness (R_a) of about 8 nm (measured with optical profilometry, Wyko NT-110). Prior to deposition, the substrates were ultrasonically cleaned in acetone and ethanol for 5 min each. The coatings were deposited with a self-assembled vacuum deposition unit (Fraunhofer IWM, Halle) by reactive r.f. sputtering (13.56 kHz) utilising a 4-inch silicon target and an Ar/N_2 gas mixture. Several process parameters were varied in order to optimise the coating composition, microstructure, etc., see Table 1. Based on the theoretical results, two of the coatings were doped using C by introducing ethylene (C_2H_4) gas into the chamber as a reactive agent. All substrates were heated during deposition, except for coating no. 2. One CoCr substrate sample and one Si-wafer were coated in each process. In some of the coating processes, the Si-wafer accidentally tilted and these samples were not further analysed. To avoid overheating of the target, the coating process alternated between 10 min sputtering and 3 min breaks. The total deposition time was 2 h, except coating no. 3 which had a deposition time of 3 h.

2.3 Coating characterisation

The coating morphology and thickness were examined on fracture cross-sections in the scanning electron microscope (SEM, LEO 1550). To prevent charging in the SEM, a thin layer of Au/Pd was sputter-coated on top of the PVD coatings. SEM was also utilised to examine the wear-tracks and scratches from the tribological experiments. The coating hardness was measured with an ultra nano hardness tester (CSM Instruments UNHT) equipped with a Berkovich tip. The indents had a depth of 50 nm and 30 indents were made on each coating. As references,

Table 1 Parameters during coating processes

Coating no.	Substrate	Ar flow rate (sccm)	N ₂ flow rate (sccm)	Process pressure (Pa)	T (°C)	C ₂ H ₄ flow rate (sccm)	Power (W)
1	– CoCr	10	30	1.0	280	–	300
2	Si CoCr	10	30	1.0	25	–	300
3	Si CoCr	10	30	1.0	280	–	150
4	Si CoCr	10	30	0.5	280	–	300
5	Si CoCr	10	30	1.5	280	–	300
6	– CoCr	30	15	1.0	280	–	300
7	– CoCr	20	20	1.0	280	–	300
8	Si CoCr	20	20	1.5	280	–	300
9	Si –	20	20	0.5	280	–	300
10	Si CoCr	10	30	1.3	280	1.5	300
11	Si CoCr	10	30	1.3	280	0.5	300

hardness was also measured on the CoCr substrate surface and on bulk silicon nitride (Si₃N₄). The indentations were analysed in accordance with the Oliver–Pharr method [27]. The statistical evaluation of the hardness measurements was done using IBM SPSS 19.1 (SPSS Inc, Chicago, IL), a one-way ANOVA was used with Scheffé's test for multiple comparisons. Probability (*P*) values were considered significant if below 0.05. Chemical analyses were performed with energy dispersive X-ray spectroscopy (EDS) using an acceleration voltage of 10 kV. The phase compositions of the coatings were analysed using grazing incidence X-ray diffraction (GIXRD) (Siemens D5000), performed with fixed incident angle at 1° using CuK α radiation. The surface roughness of the coatings as well as the wear-track cross sectional areas were analysed by light interference microscopy utilising a Wyko NT-110 in phase shift interferometry mode (PSI) and vertical scanning interferometry mode (VSI). The coating microstructure was analysed with transmission electron microscopy (TEM) by a FEI Tecnai F30 ST TEM. The TEM-sample was prepared using a dual-beam FIB/SEM (FEI DB235, FEI Company, The Netherlands) using the in situ lift-out technique.

2.4 Tribological testing

The coatings are aimed to be used in metal on metal total joint replacements. In this paper, the hip joint was simulated using a ball-on-disc apparatus [28]. The coated substrates were slid against a stationary polished ball of Si₃N₄ (representing a coated counter surface) with a diameter of 6 mm while the friction was continuously measured. The sliding speed was held to 0.04 m/s with a track radius of 2.5 mm. The normal load was 1 N. The corresponding maximum Hertzian pressure [29] can then be estimated to 0.76 GPa, assuming contact between a Si₃N₄ ball (320 GPa, Poisson's ratio 0.27) and CoCr flat (241 GPa, Poisson's ratio 0.3), and neglecting the influence from the

coating. This would correspond to a load of 545 kN on a hip joint with a head diameter of 28 mm and a radial clearance to the cup of 100 μ m, assuming both head and cup are made of the CoCr steel, and again neglecting the small influence from the thin coating on the contact pressure. All tests were carried out in a bovine serum solution (25 % serum) which was prepared in accordance with the ASTM standard [30]. Two tests were performed on each sample at 1,000 and 10,000 revolutions respectively. Note that the contact pressure is much higher than the average pressures in a joint, and that the continuous directional sliding in the ball-on-disc test is quite far from the complex motion of a hip joint. The results can therefore only be used as preliminary indications, rather than for predicting the performance in vivo. A specific wear rate was determined according to: Specific wear rate (mm³/Nm) = Wear volume (mm³)/[Load (N) \times Sliding distance (m)]. The wear rate of the coatings and reference materials, excluding the ball, was calculated as worn cross-sectional area times the diameter of the wear track. Note that when comparing wear rates with other studies, as for all tribological testing, care needs to be taken, since there are many parameters that can affect the wear rate.

In order to analyse the fracture mechanisms and adhesion of the coating, scratch tests were performed using a Rockwell C diamond with a tip radius of 200 μ m. Two 10 mm scratches were made on each coated CoCr sample, with a sliding velocity of 5 mm/min and a load starting from 0 N and continuously increasing by 50 N/min.

3 Results

3.1 Theoretical calculations

The effect of substitutional C on the structural stability of Si₃N₄ has been calculated for four different C

concentrations. Si was replaced by C to 0, 2, 3, and 5 % of the total number of atoms in the system. The resulting formation energies were related to the corresponding energy for pure Si_3N_4 (i.e. 0 % C). It was obvious that the process of replacing Si with C is endothermic, and that this endothermic value will increase drastically with an increase in C concentration; +220 (2 %), +471 (3 %) versus +703 (5) kJ/mol. Hence, the C dopant will destabilize bulk Si_3N_4 . The effect of substitutional C on the surface reactivity of Si_3N_4 has also been calculated for four different C concentrations (0, 1, 3, and 4 %). The adsorption energy for H (or OH) adsorbed to Si on a non-doped Si_3N_4 surface has been calculated to $-408/-621$ kJ/mol (it is as expected an exothermic process). The C incorporation into the lattice resulted in either an increased, or decreased, surface reactivity—as measured by the calculated adsorption energy for H or OH ($-439/-477$ (1 %), $-452/-540$ (3 %) vs. $-479/-660$ (4 %) kJ/mol). As can be seen from these results, the surface reactivity is affected not only by the presence of C in the structure, but also of the concentration of this dopant element. It is also apparent that the adsorption situation depends on the adsorbed species (H or OH in this case). The general result is that the surface reactivity will increase with an increased concentration of C in the structure. However, C will improve the adsorption of H for all C concentrations. In summary, fragments of Si_3N_4 will be largely destabilized by higher concentrations of dopant C. In addition, these higher concentrations of C will cause a more pronounced surface reactivity (true for both the bearing surfaces and the wear particles).

3.2 Coatings

Almost all the Si_xN_y -coatings exhibited a fine surface nanostructure, as exemplified in Fig. 1a. The only exception was coating no. 2 (deposited with a lower substrate temperature), which showed thin coating patches, Fig. 1b. The surface roughness (R_a) of coating no. 2 is about 250 nm, while for the other coatings it is about 5 nm on Si substrates and 10 nm on CoCr substrates. This corresponds to an R_a of about 3 and 8 nm for the Si and CoCr substrates, respectively, prior to coating deposition.

The cross sections of the coatings on Si-substrate show different structures, as shown in Fig. 2. Coatings no. 5 and 8 (Figs. 2a, b) have a columnar structure and a thickness of approximately 1.4 μm . Coating no. 3 (Fig. 2c) that was deposited with lower target power has a structure similar to coatings no. 5 and 8 but with finer columns and coating thickness about 600 nm. Coating no. 10 (Fig. 2d) deposited with C_2H_4 , is approximately 1.2 μm thick and has a much coarser but less columnar microstructure than coatings 3, 5, and 8. All coatings have a typical thickness, determined from cross-sections, of 1.0–1.7 μm and a

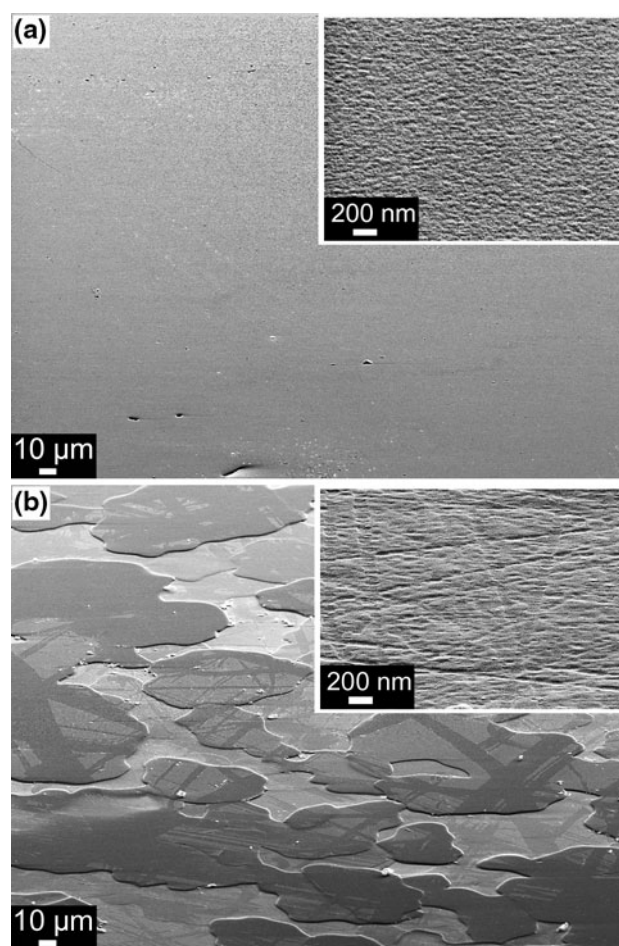


Fig. 1 Surface appearance of coatings at two magnifications. SEM, 67° sample tilt; **a** coating no. 5 on Si-substrate; **b** coating no. 2 on CoCr substrate

deposition rate of 0.2–0.3 nm/s. Coating no. 3 is an exception and has a deposition rate of 0.07 nm/s. The thickness also varied within individual samples, due to the decreasing deposition rate from the centre below the target towards the periphery.

The quantitative EDS analysis showed that the N/Si ratio for the coatings was about 1.5 (± 0.3), which is slightly higher than 1.33 for stoichiometric Si_3N_4 . No clear correlations were found between the N/Si ratios and the argon and nitrogen flow during the coating process. Coating no. 10, which was deposited with C_2H_4 introduced into the chamber, had about the same carbon content as the rest of the coatings, i.e. 3–5 %.

No crystalline structure in the coatings was detected by XRD, Fig. 3. The only observed crystalline reflections could be indexed to Co, Cr and Co_3Mo [31–33]. However, a marked amorphous bump was observed originating from the coating (especially for no. 8) at 20°–35°, see Fig. 3.

Selected area electron diffraction (SAED) in the TEM produced ring-like patterns with sharp dark speckles,

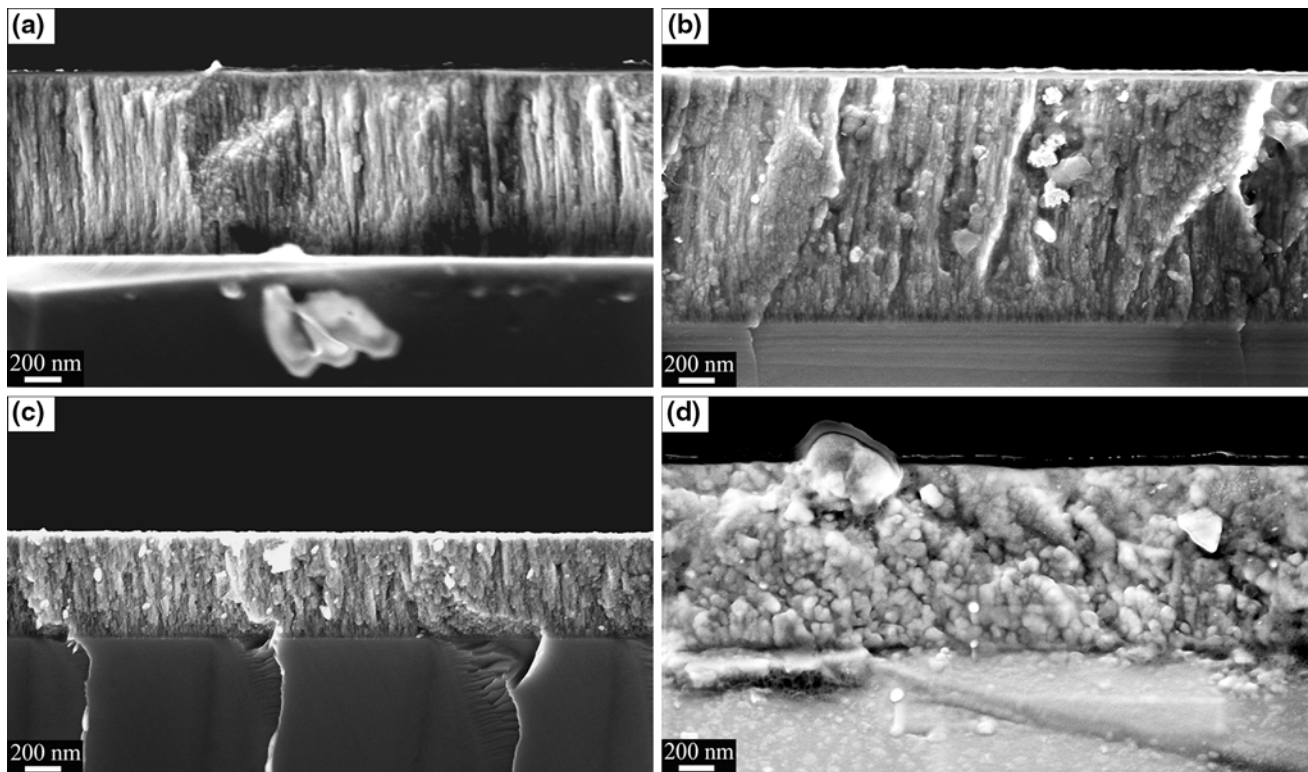


Fig. 2 Cross sections of coatings on silicon wafers showing the resulting microstructures. The superficial thin layer on top is the metal film deposited to avoid charging in the SEM. **a** Coating no. 5 showing

representing a nanocrystalline structure, Fig. 4a. Via indexing, it was evident that all rings represented Si_3N_4 . Furthermore, the high resolution TEM images exhibit lattice fringes consistent with a polycrystalline material, Fig. 4b.

The hardness of the Si_xN_y -coatings was in the same range as the superficial hardness of bulk silicon nitride ($P = 0.08\text{--}1$), except for coating no. 8 on both CoCr and Si, which was significantly softer than bulk silicon nitride ($P < 0.01$). All coatings, as well as bulk silicon nitride were harder than bulk CoCr, see Table 2 ($P < 0.001$). In five cases out of six, the coatings on the silicon wafers had a mean hardness slightly lower than that of the coatings on the CoCr substrates. However, that difference was only statistically significant (at a significance level of $\alpha = 0.05$) for coating no. 2. Coating no. 11 flaked off before the hardness test.

The scratch tests gave an indication of the relative adhesion of the coatings. Most of the coatings flaked off immediately when the scratch tip touched the surface so the critical load, i.e. the starting point of continuous delamination, was 0 N, see Table 2. Coating no. 5 (Fig. 5a) that flaked off during the ball-on-disc test also cracked and flaked off immediately when the scratch tip hit the surface, while coating no. 8 (Fig. 5b) showed a critical load of approximately 7 N.

a columnar structure; **b** coating no. 8 showing a columnar structure; **c** coating no. 3 showing a fine columnar structure; **d** coating no. 10 without a distinct columnar structure

3.3 Friction

For most of the ball-on-disc friction measurements, no distinct friction differences were revealed between the different types of coatings, and bulk CoCr, Fig. 6. The major part of the coatings had a coefficient of friction between 0.12 and 0.22, indicated by the grey area in Fig. 6. However, for coating no. 5 it increased up to 0.45 when the coating flaked off. Coating no. 2 with a rougher surface had a constant coefficient of friction at about 0.31. Almost all tests started with a relatively fast and short friction decrease and then a longer increase stabilising after about 1,000 revolutions. The average friction coefficient after the running-in time is given in Table 2. The test with bulk Si_3N_4 exhibited a slow decrease starting at about 1,000 revolutions which lasted throughout the entire test.

3.4 Wear of coating surfaces

The coating topography was gradually smoothed out during sliding against the Si_3N_4 -ball in the bovine serum solution, as exemplified by coating no. 8 in Fig. 7a, b. In general, the same type of wear was demonstrated on the coatings on CoCr substrates as on the Si substrates. However, some of the coatings on CoCr substrate (no. 6, 7, and 11) flaked off before the ball-on-disc tests. Coating no. 5 on CoCr

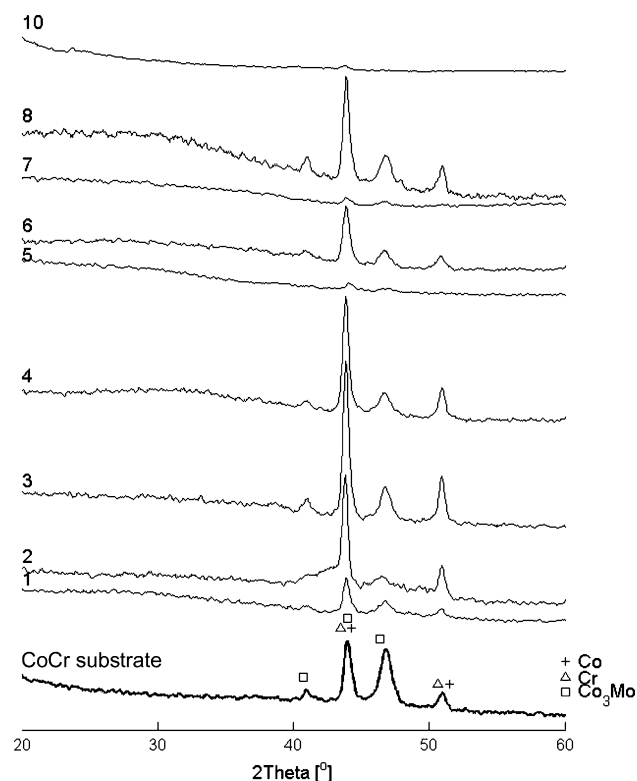


Fig. 3 GI-XRD of Si_xN_y -coatings 1–8 on CoCr substrates and uncoated CoCr substrate with designated peaks

cracked and flaked off in the wear-track during testing, Fig. 8a, whereas the coating on Si seemed to have better adhesion and the wear-track was just smoothed out, Fig. 8b. Further, parts of the wear-track for coating no. 3 flaked off during the 1,000 revolutions test but the remaining coating then withstood the whole 10,000 revolutions test. The flaking off was probably initiated by the randomly distributed defects noted on several coatings. The widths of the wear-tracks that did not flake off were about $90\ \mu\text{m}$, this holds for coatings both on CoCr and Si substrates. The bulk Si_3N_4 , which had an initial roughness (R_a) of $15\ \text{nm}$, higher than that of the coatings, seemed to be less worn. The wear-track displayed some grooves, but no other indications of wear were visible, see Fig. 9. The wear-track on bulk CoCr was much wider than those of the coatings and bulk Si_3N_4 , it also had distinct grooves around the entire wear-track, Fig. 10.

All coatings that did not flake off showed a good wear resistance, almost matching that of the bulk Si_3N_4 , see Fig. 11. The specific wear rate was approximately $1 \times 10^{-7}\ \text{mm}^3/\text{Nm}$ for bulk Si_3N_4 and for certain coatings (no. 1, 3, 4, 8, and 10), about $3 \times 10^{-7}\ \text{mm}^3/\text{Nm}$, (Table 2). The uncoated CoCr showed much lower wear resistance, with a specific wear rate of about $60 \times 10^{-7}\ \text{mm}^3/\text{Nm}$.

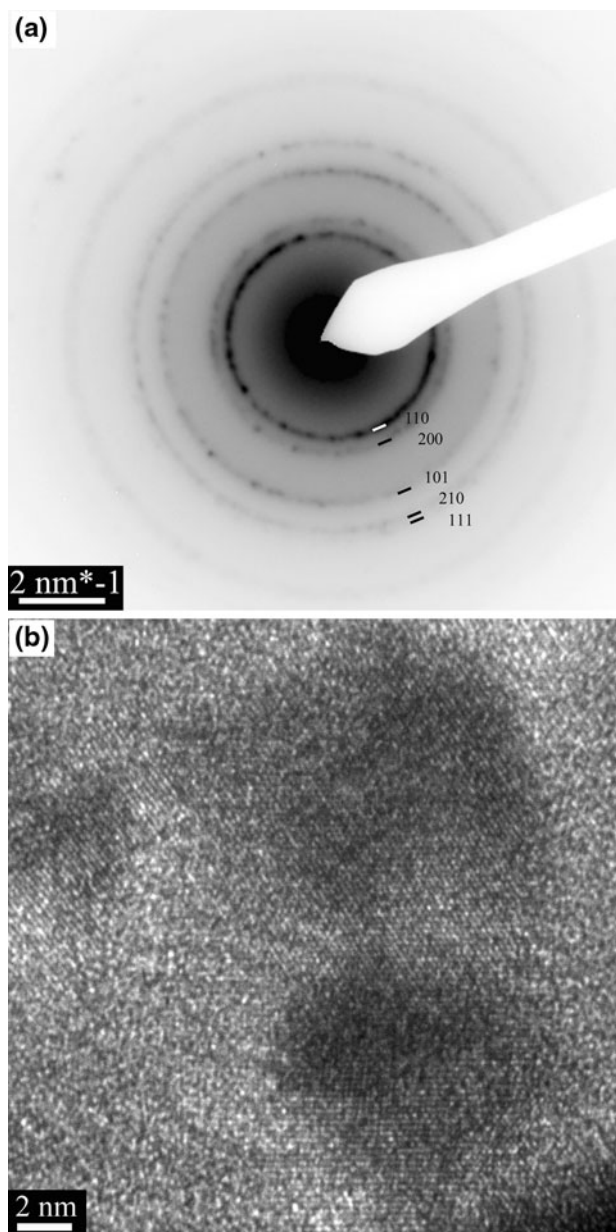


Fig. 4 TEM diffraction pattern and images of coating no. 8; **a** SAED pattern indicating Si_3N_4 ; **b** high resolution TEM image of Si_3N_4 lattice within the coating

4 Discussion

Despite the variation of several deposition parameters, not much difference in the chemical composition, phase composition, nanostructure, or tribological properties of the resulting coatings was found. According to EDS, the N/Si ratio of the coatings was higher than that of Si_3N_4 , which might imply that the Si was saturated with N and that the nitrogen flow would have to be lowered to achieve stoichiometric Si_3N_4 . Further, the carbon content was unaffected for coatings no. 10 and 11, which were deposited

Table 2 Coatings 1–11 and bulk material (CoCr and Si₃N₄) characteristics in terms of microstructural and mechanical properties

Coating no. or reference material Substrate	Surface roughness (nm) CoCr	Coating thickness (μm) Si	Mean hardness (±SD) (GPa) CoCr	Mean hardness (±SD) (GPa) Si	Critical load scratch test (N) CoCr	Friction coefficient after running-in CoCr	Specific wear rate (mm ³ /Nm) (1 N, n = 10,000) CoCr
1	10	**	21.5 (±2.7)	**	0	0.15	3.0 × 10 ⁻⁷
2	250	1.7	24.2 (±3.0)	20.4 (±2.6)	2	0.31	–
3	10	0.6	21.2 (±2.0)	20.5 (±2.3)	4	0.19	2.7 × 10 ⁻⁷
4	10	1.1	22.3 (±2.5)	21.5 (±2.9)	2	0.13	3.2 × 10 ⁻⁷
5	10	1.4	22.1 (±2.5)	19.7 (±2.0)	0	***	***
6	10	**	21.6 (±4.2)	**	0	***	***
7	10	**	22.5 (±2.9)	**	0	***	***
8	10	1.4	18.0 (±2.2)	19.0 (±1.8)	7	0.17	3.2 × 10 ⁻⁷
9 *	*	1.0	*	22.5 (±2.7)	*	*	*
10	10	1.2	21.6 (±3.7)	21.4 (±2.2)	3	0.16	3.0 × 10 ⁻⁷
11	10	1.1	***	***	***	***	***
CoCr	8		8.5 (±0.9)			0.18	60 × 10 ⁻⁷
Si ₃ N ₄	15		23.4 (±2.6)			0.13	1.0 × 10 ⁻⁷

* Only on Si substrate
 ** Only on CoCr substrate
 *** Flaked off before the test

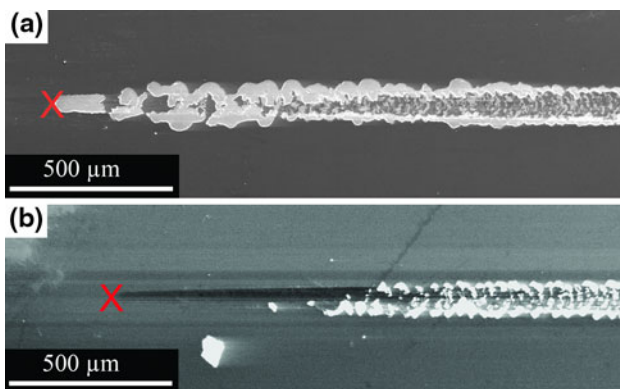


Fig. 5 Surface appearance after scratch test of coatings on CoCr substrates. SEM, 0° sample tilt. The start of the scratch is indicated with an X; **a** coating no. 5, showing immediate flaking off; **b** coating no. 8, showing continuous delamination for loads exceeding approximately 7 N

with a C₂H₄ flow in the chamber. This is in agreement with earlier work by Li et al. [34] who also sputtered Si₃N₄ with ethylene in the chamber. It should be added that coating no. 11 flaked off before any of the tests or analyses were performed.

Two deposition parameters showed a notable impact on the coating properties, i.e. target power and substrate temperature. For a lower target power, 150 W for coating no. 3, the deposition rate was more than halved (0.07 nm/s) compared to coatings deposited with 300 W (0.2–0.3 nm/s), resulting in a thinner coating. A lower substrate temperature,

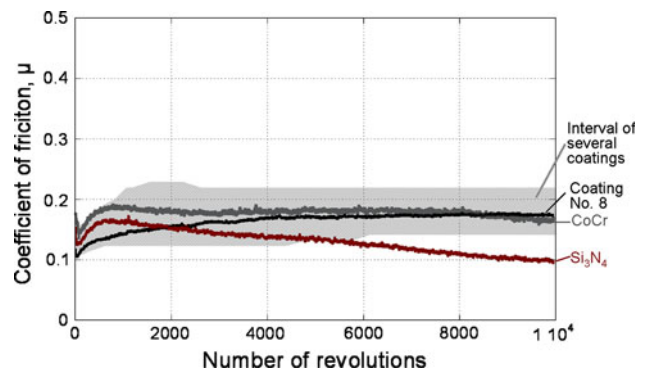


Fig. 6 Coefficient of friction versus number of revolutions for Si_xN_y-balls sliding against the different Si_xN_y-coatings and bulk CoCr and bulk Si₃N₄. The gray area represents the region containing all the coating curves for no. 1, 3, 4, and 10

as for coating no. 2, resulted in a rougher surface. For all other coatings the roughness was in the range of that found on conventional implants [35, 36]. The higher roughness of coating no. 2 was coupled to the patched character. Within the individual patches the roughness was similar to the other coatings. The patches most likely appear due to flaking during the cyclic deposition process, since individual patches are approximately 0.2 μm thick while the full coating is 1.5 μm thick.

Interestingly, the coatings seemed amorphous in the XRD, whereas TEM studies revealed nanocrystallinity. This is in line with the Scherrer equation [37], saying that

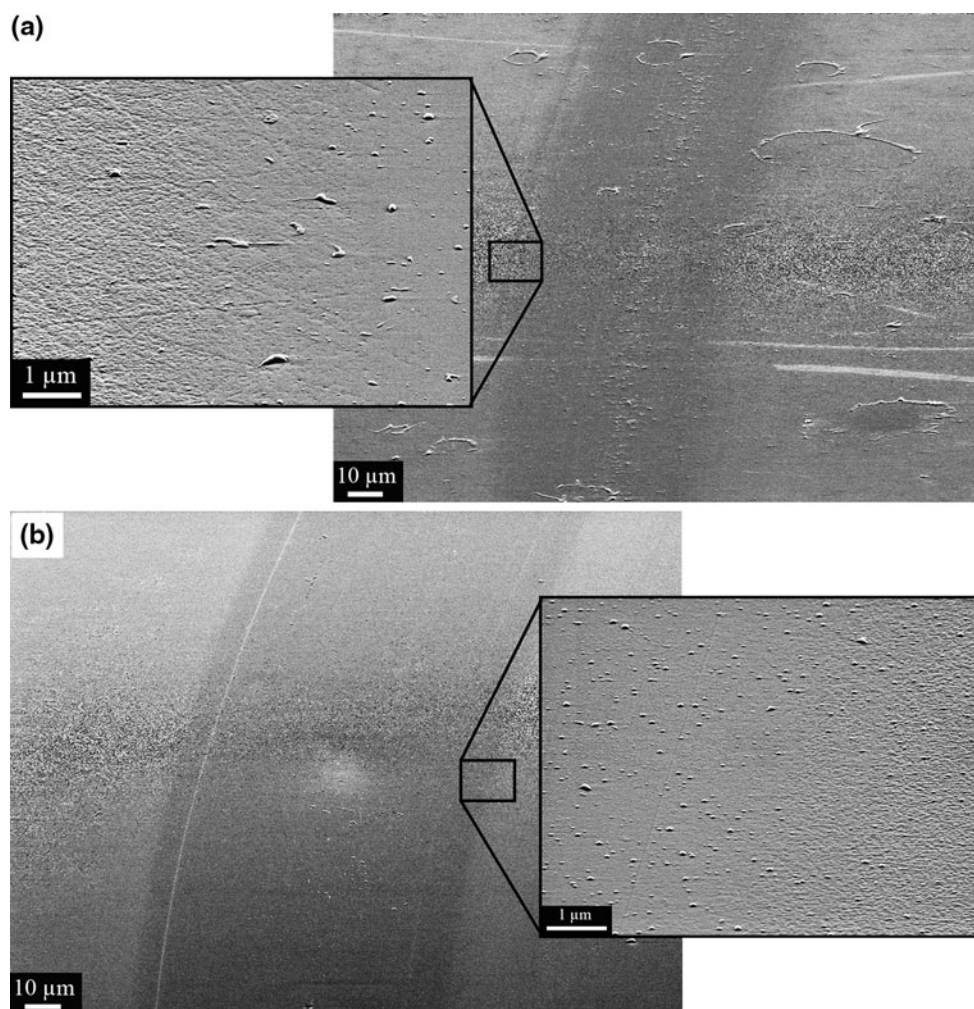


Fig. 7 Surface appearance of the wear-tracks on coating no. 8 after 10,000 revolutions. The coating is smoothed out in the wear-tracks. SEM, 67° sample tilt. *Insets* show detail at higher magnification; **a** coating no. 8 deposited on CoCr substrate; **b** coating no. 8 deposited on Si substrate

diffraction peaks in XRD broaden with decreasing size of the crystal. Obviously, the TEM is needed to reveal the structures of the coatings, ranging from amorphous to nanocrystalline.

The hardness of the coatings was similar to that of bulk Si_3N_4 , except for coating no. 8, which had a hardness below 20 GPa. The hardness of PVD coatings may be affected by chemical composition, chemical structure, and microstructure [38, 39]. However, in this case no such differences could be found. For all the coatings except no. 8, the hardness on CoCr substrates was higher than on Si substrates. Si has a low thermal expansion compared to metals [40] and the difference in thermal expansion is higher between CoCr and the coating material than between Si and the coating material. Compressive stresses of the coatings are induced when the samples are cooled after deposition due to the higher thermal expansion of the substrate [38, 41]. Compressive residual stresses contribute to higher hardness of the coating [38], which might explain

the higher hardness of the coatings on CoCr. High compressive stresses also weaken the adhesion of coatings [41], which has been an issue for this coating series. The slightly lower hardness of coating no. 8 could not be explained by the deposition parameters nor the microstructure. Harder coatings with similar microstructure and deposition parameters do not appear to differ from coating no. 8, see Fig. 2a, b. Other, slightly different microstructures, for example those of coating no. 3 and 10 (Fig. 2b, c), do not appear to affect the hardness.

As in a previous investigation by the present authors [11], the coefficient of friction was at about the same level in the serum solution, despite differences in material combinations and amount of wear of the surfaces. The previous investigation showed that the friction was strongly dependent on the carbon tribofilm which often forms on the sliding surfaces in bovine serum [11]. The friction level and wear rate found in the present study are comparable to those of a similar study on a Si_3N_4 -TiN composite [42].

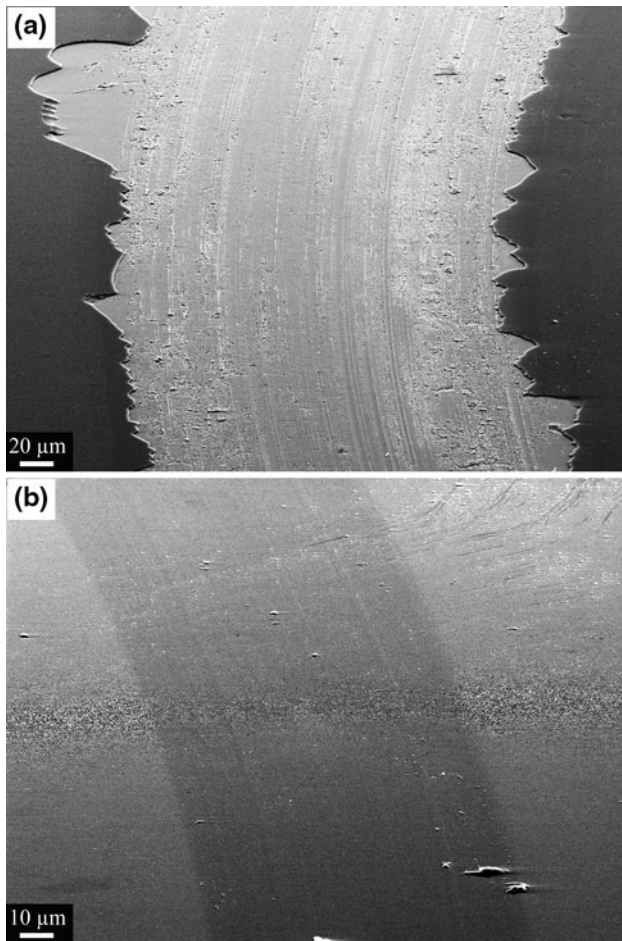


Fig. 8 Surface appearance of the wear-tracks on coating no. 5. SEM, 67° sample tilt; **a** after 1,000 revolutions the coating deposited on CoCr substrate has flaked off in the entire wear-track; **b** after 10,000 revolutions the coating deposited on Si substrate has just been smoothed out

The wear rate for CoCr in this study is much lower than for another study, probably since they used a higher contact pressure [43]. Somewhat contradicting is a hip simulator

Fig. 9 Surface appearance of the wear-track on bulk Si₃N₄ after 10,000 revolutions showing some porosity. SEM at two different magnifications, 67° sample tilt

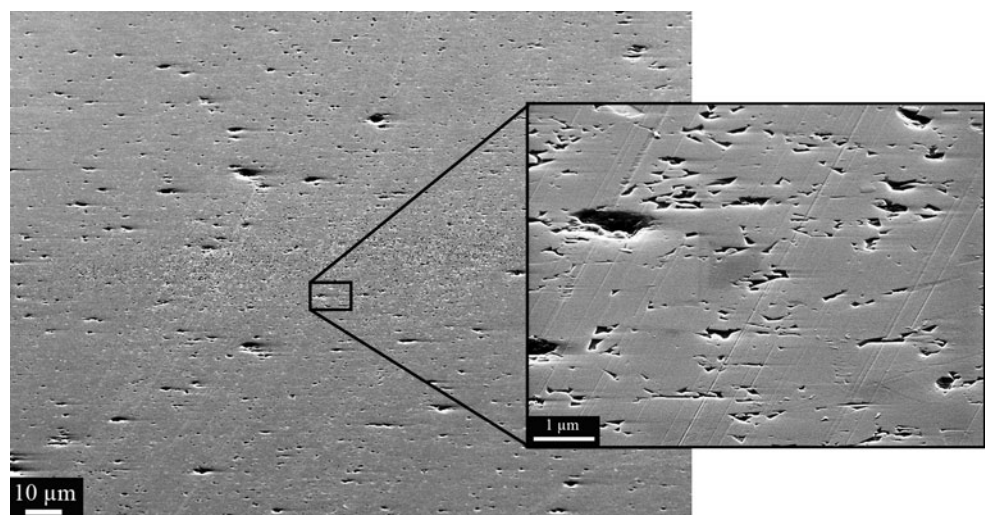


Fig. 10 Surface appearance of the wear-track on bulk CoCr sample after 10,000 revolutions where distinct grooves follow the entire wear-track. SEM, 67° sample tilt

study showing wear volumes in a similar range as in the current study, but slightly lower wear for Si₃N₄ on CoCr than for Si₃N₄ on Si₃N₄ bearing [10]. However, both bearings still have significantly lower wear than CoCr on CoCr and CoCr on UHMWPE. Note that a hip simulator study may differ in many ways from a screening test and the resulting wear can therefore differ [44]. In perspective of other coatings (TiN, CrN, and CrCN) tested in a similar manner, the SiN coatings show promising wear resistance [18].

The theoretical calculations revealed that the chemical stability and surface reactivity of a Si₃N₄-coating could be controlled by the amount of dopant C. The amount of C should be chosen to get a material that is chemically stable as a coating but when the surface area to volume ratio increases (as for small wear particles) the material dissolves in vivo. With the present coating processes, it proved hard to vary the amount of C. However, it is likely

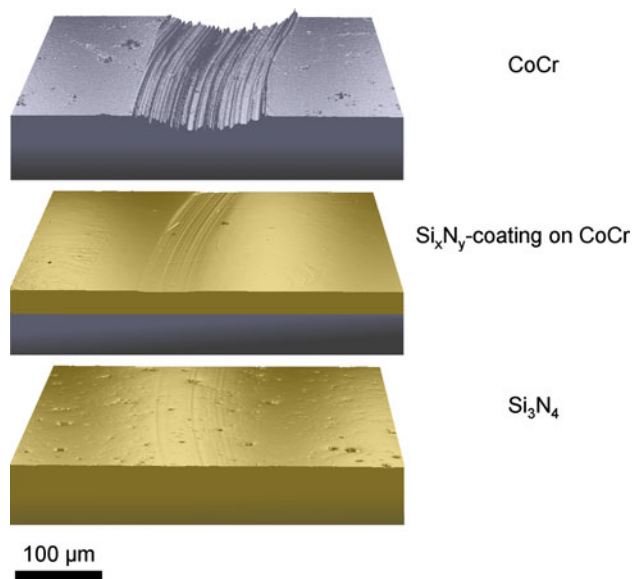


Fig. 11 Optical profile images of worn surfaces and the cross-sectional areas of the wear-tracks. The z -scale is magnified 23 times more than the x and y scales

that control of the chemical stability could be improved by using co-sputtering with an additional target of C.

The limiting factor of manufactured coatings is the adhesion to the substrates which could be improved in future experiments by lowering the substrate temperature, sputtering of an inter-layer and sputter cleaning of the substrates prior to deposition.

The low wear rate demonstrates the potential of these coatings for use on bearing surfaces of joints, since it translates to a low amount of wear particles that could cause inflammation leading to bone loss and implant loosening [1–3]. The risk of implant loosening is further reduced due to the dissolution of the wear particles. The system also has the advantage of having a sort of redundancy. If the coatings eventually become worn out or flake off, the substrates that become exposed should still be able to give good functionality, since they consist of the traditional metal on metal combination for joint implants.

5 Conclusions

PVD-coatings of Si_xN_y have been reactively deposited and evaluated as an alternative contact surface for total joint replacements. The surface appearance, chemical composition, phase composition, nanostructure, and coating hardness were analysed. The coated samples were tribologically tested in a ball-on-disc apparatus and compared with bulk CoCr and bulk Si_3N_4 .

DFT calculations showed that the solubility and reactivity of Si_3N_4 could be controlled by the amount of dopant

C. Only two deposition parameters, substrate temperature and sputtering power, could be linked to the coating properties. The coatings were amorphous or nanocrystalline and exhibited a high hardness, similar to that of bulk Si_3N_4 . The coefficient of friction of the coatings against Si_3N_4 in serum solution was similar to that of bulk Si_3N_4 and CoCr. The low wear rates of the Si_xN_y -coating were much closer to that of bulk Si_3N_4 than that of CoCr, which suggests that a smaller quantity of wear particles would be produced at the bearing surface of the joint using these coatings. However, the adhesion of the coating must be improved.

The above results, in combination with the previously demonstrated ability of silicon nitride particles to dissolve in PBS, suggest that these types of coatings could potentially reduce the risk of implant loosening.

Acknowledgments The authors are grateful for the financial support from the Swedish Foundation for Strategic Research (SSF) Program in Materials for Nanoscale Surface Engineering (MS²E). Sandvik Materials Technology is recognised for providing substrate materials.

References

- Sargeant A, Goswami T. Hip implants: paper V. Physiological effects. *Mater Des.* 2006;27:287–307.
- Landgraeber S, von Knoch M, Löer F, Wegner A, Tsokos M, Hußmann B, Totsch M. Extrinsic and intrinsic pathways of apoptosis in aseptic loosening after total hip replacement. *Biomaterials.* 2008;29:3444–50.
- Bozic KJ, Ries MD. Wear and osteolysis in total hip arthroplasty. *Semin Arthroplasty.* 2005;16:142–52.
- Balla VK, Xue W, Bose S, Bandyopadhyay A. Laser-assisted Zr/ZrO₂ coating on Ti for load-bearing implants. *Acta Biomater.* 2009;5:2800–9.
- Derbyshire B, Fisher J, Dowson D, Hardaker C, Brummitt K. Comparative study of the wear of UHMWPE with zirconia ceramic and stainless steel femoral heads in artificial hip joints. *Med Eng Phys.* 1994;16:229–36.
- Sargeant A, Goswami T. Hip implants—paper VI—ion concentrations. *Mater Des.* 2007;28:155–71.
- Bizot P, Sedel L. Alumina bearings in hip replacement: theoretical and practical aspects. *Oper Tech Orthop.* 2001;11:263–9.
- Willmann G, Früh HJ, Pfaff HG. Wear characteristics of sliding pairs of zirconia (Y-TZP) for hip endoprostheses. *Biomaterials.* 1996;17:2157–62.
- Jahanmir S. Friction and wear of ceramics. New York: Marcel Dekker, Inc.; 1994. p. 313–7.
- Bal BS, Khandkar A, Lakshminarayanan R, Clarke I, Hoffman AA, Rahaman MN. Fabrication and testing of silicon nitride bearings in total hip arthroplasty: winner of the 2007 “HAP” Paul award. *J Arthroplasty.* 2009;24:110–6.
- Olofsson J, Grehk TM, Berling T, Persson C, Jacobson S, Engqvist H. Evaluation of silicon nitride as a wear resistant and resorbable alternative for total hip joint replacement. *Biomater.* 2012;2:1–9.
- Guedes e Silva CC, Higa OZ, Bressiani JC. Cytotoxic evaluation of silicon nitride-based ceramics. *Mater Sci Eng C.* 2004;24:643–6.

13. Xu J, Kato K. Formation of tribochemical layer of ceramics sliding in water and its role for low friction. *Wear*. 2000;245: 61–75.
14. Tomizawa H, Fischer TE. Friction and wear of silicon nitride and silicon carbide in water: hydrodynamic lubrication at low sliding speed obtained by tribochemical wear. *ASLE Trans*. 1986;30: 41–6.
15. Österle W, Klaffke D, Griepentrog M, Gross U, Kranz I, Knabe C. Potential of wear resistant coatings on Ti-6Al-4 V for artificial hip joint bearing surfaces. *Wear*. 2008;264:505–17.
16. Yen SK, Guo MJ, Zan HZ. Characterization of electrolytic ZrO₂ coating on Co–Cr–Mo implant alloys of hip prosthesis. *Biomaterials*. 2001;22:125–33.
17. Fisher J, Hu X, Tipper J, Stewart T, Williams S, Stone M, Davies C, Hatto P, Bolton J, Riley M, Hardaker C, Isaac G, Berry G, Ingham E. An in vitro study of the reduction in wear of metal-on-metal hip prostheses using surface-engineered femoral heads. *Proc Inst Mech Eng*. 2002;216:219–30.
18. Williams S, Tipper JL, Ingham E, Stone MH, Fisher J. In vitro analysis of the wear, wear debris and biological activity of surface-engineered coatings for use in metal-on-metal total hip replacements. *Proc Inst Mech Eng*. 2003;217:155–63.
19. Wang RR, Welsch GE, Monteiro O. Silicon nitride coating on titanium to enable titanium–ceramic bonding. *J Biomed Mater Res*. 1999;46:262–70.
20. Matsuoka M, Isotani S, Sucasaire W, Zambom LS, Ogata K. Chemical bonding and composition of silicon nitride films prepared by inductively coupled plasma chemical vapor deposition. *Surf Coat Technol*. 2010;204:2923–7.
21. Qian F, Temmel G, Schnupp R, Ryssel H. Thin stoichiometric silicon nitride prepared by r.f. reactive sputtering. *Microelectron Reliab*. 1999;39:317–23.
22. Lattemann M, Nold E, Ulrich S, Leiste H, Holleck H. Investigation and characterisation of silicon nitride and silicon carbide thin films. *Surf Coat Technol*. 2003;174–175:365–9.
23. Ku S-L, Lee C-C. Surface characterization and properties of silicon nitride films prepared by ion-assisted deposition. *Surf Coat Technol*. 2010;204:3234–7.
24. Heimann RB. Thermal spraying of silicon nitride coatings using highly accelerated precursor powder particles. *Surf Coat Technol*. 2010;205:943–8.
25. Perdew JP, Wang Y. Accurate and simple analytic representation of the electron–gas correlation energy. *Phys Rev B*. 1992;45: 13244.
26. Monkhorst HJ, Pack JD. On special points for brillouin zone integrations. *Phys Rev B*. 1976;13:5188–92.
27. Oliver WC, Pharr GM. An improved technique for determining hardness and elastic modulus using load and displacement sensing indentation experiments. *J Mater Res*. 1992;7:1564–83.
28. Czichos H, Becker S, Lexow J. International multilaboratory sliding wear tests with ceramics and steel. *Wear*. 1989;135: 171–91.
29. Johnson KL. *Contact mechanics*. Cambridge: The Press Syndicate of the University of Cambridge; 1985. p. 90–104.
30. ASTM and Standards. Standard test for wear testing of polymeric materials used in total joint prostheses. *ASTM Int. F 732-00*; (2003).
31. International Centre for Diffraction Data, Reference files: Cobalt PDF no. 15-0806.
32. International Centre for Diffraction Data, Reference files: Chromium PDF no. 88-2323.
33. International Centre for Diffraction Data, Reference files: Cobalt Molybdenum PDF no. 29-0488.
34. Li G, Li Y, Li G. Crystallization of amorphous Si₃N₄ and superhardness effect in HfC/Si₃N₄ nanomultilayers. *Appl Surf Sci*. 2011;257:5799–802.
35. Kim Y-HA, Ritchie A, Hardaker C. Surface roughness of ceramic femoral heads after in vivo transfer of metal: correlation to polyethylene wear. *J Bone Joint Surg*. 2005;87:577–82.
36. Fisher J, Jennings L, Galvin A. Wear of highly crosslinked polyethylene against cobalt chrome and ceramic femoral heads. In: Benazzo F, Falez F, Dietrich M, editors. *Bioceramics and alternative bearings in joint arthroplasty*. Dramstadt: Steinkopff Verlag; 2006. p. 185–8.
37. Klug DHP, Alexander LE. *X-ray diffraction procedures for polycrystalline and amorphous materials*. New York: Wiley. Inc; 1954. p. 491.
38. Karlsson L, Hultman L, Sundgren JE. Influence of residual stresses on the mechanical properties of TiC_xN_{1-x} (x = 0, 0.15, 0.45) thin films deposited by arc evaporation. *Thin Solid Films*. 2000;371:167–77.
39. Wen M, Meng QN, Yu WX, Zheng WT, Mao SX, Hua MJ. Growth, stress and hardness of reactively sputtered tungsten nitride thin films. *Surf Coat Technol*. 2010;205:1953–61.
40. Nordling L, Östeman J. *Physics handbook for science and engineering*. Vol. 5. Lund: Studentlitteratur; 1980.
41. Wiklund U, Gunnars J, Hogmark S. Influence of residual stresses on fracture and delamination of thin hard coatings. *Wear*. 1999; 232:262–9.
42. Mazzocchi M, Gardini D, Traverso P, Faga M, Bellosi A. On the possibility of silicon nitride as a ceramic for structural orthopaedic implants. Part II: chemical stability and wear resistance in body environment. *J Mater Sci Mater Med*. 2008;19:2889–901.
43. Spriano S, Vernè E, Faga MG, Bugliosi S, Maina G. Surface treatment on an implant cobalt alloy for high biocompatibility and wear resistance. *Wear*. 2005;259:919–25.
44. Affatato S, Spinelli M, Zavalloni M, Mazzega-Fabbro C, Viceconti M. Tribology and total hip joint replacement: current concepts in mechanical simulation. *Med Eng Phys*. 2008;30: 1305–17.